Cellular/Molecular

Activation of Presynaptic GABA$_{B(1a,2)}$ Receptors Inhibits Synaptic Transmission at Mammalian Inhibitory Cholinergic Olivocochlear–Hair Cell Synapses

Carolina Wedemeyer,[1] Javier Zorrilla de San Martín,[1] Jimena Ballestero,[1] María Eugenia Gómez-Casati,[1,2] Ana Vanesa Torbidoni,[1] Paul A. Fuchs,[3] Bernhard Bettler,[4] Ana Belén Elgoyhen,[1,2]* and Eleonora Katz[1,5]*

[1]Instituto de Investigaciones en Ingeniería Genética y Biología Molecular "Dr. Héctor N. Torres," 1428 Buenos Aires, Argentina, [2]Tercera Cátedra de Farmacología, Facultad de Medicina, 1121 Buenos Aires, Argentina, [3]Johns Hopkins University, School of Medicine, Baltimore, Maryland 21205, [4]Department of Biomedicine, Institute of Physiology, University of Basel, CH-4056 Basel, Switzerland, and [5]Departamento de Fisiología, Biología Molecular y Celular, Facultad de Ciencias Exactas y Naturales, Universidad de Buenos Aires, 1428 Buenos Aires, Argentina

The synapse between olivocochlear (OC) neurons and cochlear mechanosensory hair cells is cholinergic, fast, and inhibitory. The inhibitory sign of this cholinergic synapse is accounted for by the activation of Ca^{2+}-permeable postsynaptic $\alpha9\alpha10$ nicotinic receptors coupled to the opening of hyperpolarizing Ca^{2+}-activated small-conductance type 2 (SK2)K$^+$ channels. Acetylcholine (ACh) release at this synapse is supported by both P/Q- and N-type voltage-gated calcium channels (VGCCs). Although the OC synapse is cholinergic, an abundant OC GABA innervation is present along the mammalian cochlea. The role of this neurotransmitter at the OC efferent innervation, however, is for the most part unknown. We show that GABA fails to evoke fast postsynaptic inhibitory currents in apical developing inner and outer hair cells. However, electrical stimulation of OC efferent fibers activates presynaptic GABA$_{B(1a,2)}$ receptors [GABA$_{B(1a,2)}$Rs] that downregulate the amount of ACh released at the OC–hair cell synapse, by inhibiting P/Q-type VGCCs. We confirmed the expression of GABA$_B$Rs at OC terminals contacting the hair cells by coimmunostaining for GFP and synaptophysin in transgenic mice expressing GABA$_{B1}$–GFP fusion proteins. Moreover, coimmunostaining with antibodies against the GABA synthetic enzyme glutamic acid decarboxylase and synaptophysin support the idea that GABA is directly synthesized at OC terminals contacting the hair cells during development. Thus, we demonstrate for the first time a physiological role for GABA in cochlear synaptic function. In addition, our data suggest that the GABA$_{B1a}$ isoform selectively inhibits release at efferent cholinergic synapses.

Introduction

In the mammalian inner ear, hair cells convert sound into electrical signals that are conveyed to the CNS via peripheral afferent neurons. In addition, hair cells and sensory neurons receive an efferent feedback from the olivocochlear (OC) system (Guinan, 2011). This system comprises the following two groups of fibers: the medial OC (MOC) fibers, whose main targets are the outer hair cells (OHCs); and the lateral OC (LOC) fibers, mainly targeting the dendrites of type I neurons that innervate inner hair cells (IHCs; Liberman et al., 1990). The MOC system is an inhib-

itory pathway that regulates, via the MOC–OHC synapse, the cochlear amplifier. During development, IHCs are also transiently innervated by MOC fibers (Glowatzki and Fuchs, 2000; Simmons, 2002; Katz et al., 2004; Guinan, 2011; Roux et al., 2011). Before the onset of hearing, IHCs fire spontaneous action potentials that drive the release of glutamate at the first auditory synapse (Beutner and Moser, 2001). These MOC–IHC synapses might therefore play a role in the establishment of the auditory pathway, by regulating the firing frequency of IHCs during this developmental period (Glowatzki and Fuchs, 2000; Goutman et al., 2005; Johnson et al., 2011).

At MOC–hair cell synapses, acetylcholine (ACh) activates calcium-permeable $\alpha9\alpha10$ nicotinic ACh receptors (nAChRs; Elgoyhen et al., 2001) functionally coupled to the opening of calcium-dependent small-conductance type 2 (SK2) K$^+$ channels that hyperpolarize the hair cells (Dulon and Lenoir, 1996; Glowatzki and Fuchs, 2000; Oliver et al., 2000; Katz et al., 2011). ACh release is mediated by the activation of N- and P/Q-type voltage-gated calcium channel (VGCCs; Zorrilla de San Martín et al., 2010).

Although ACh is the main MOC neurotransmitter, a robust GABAergic innervation is seen both in the IHC and OHC areas (Fex and Altschuler, 1986; Vetter et al., 1991; Eybalin, 1993; Mai-

son et al., 2003). Moreover, in adult mice, GABA colocalizes with ACh in almost all efferent terminals of the OC system (Maison et al., 2003). The phenotypic analysis of mice lacking GABA_A receptor subunits has suggested that the GABAergic component of the OC system contributes to the long-term maintenance of hair cells and neurons in the inner ear (Maison et al., 2006). Furthermore, the analysis of GABA_{B1} knock-out mice has indicated that GABAergic signaling might be required for normal OHC amplifier function at low sound levels and OHC responses to high-level sound (Maison et al., 2009). In addition, GABA-mediated changes in the stiffness and motility of OHCs have been reported (Zenner et al., 1992; Batta et al., 2004). Although one study has reported that OHCs hyperpolarize in the presence of GABA (Gitter and Zenner, 1992), suggestive of the existence of postsynaptic GABA receptors, the site of action and the physiological effects of GABA at MOC–hair cell synapses are poorly understood.

To gain insight into the role of GABA in synaptic transmission at the mammalian peripheral auditory system, we searched for a postsynaptic effect of GABA at IHCs and OHCs of the developing mouse cochlea. Moreover, we studied the effect of GABA_BR-selective compounds on transmitter release at mouse MOC–hair cell synapses. Using pharmacological and electrophysiological approaches, together with mutant mouse lines lacking specific GABA_BR subtypes, we demonstrate for the first time a physiological role for GABA in OC efferent synaptic transmission. Whereas GABA does not elicit IPSCs, activation of presynaptic GABA_BRs inhibits the release of ACh from OC terminals. Thus, we demonstrate that the release of GABA at an inhibitory mammalian cholinergic synapse activates presynaptic GABA_BRs to downregulate the release of ACh.

Materials and Methods

Animal procedures and isolation of the organ of Corti. Procedures for preparing and recording from the postnatal mouse organ of Corti were essentially identical to those published previously (Glowatzki and Fuchs, 2000; Katz et al., 2004). Briefly, mid-apical turns of the organ of Corti were excised from BalbC GABA_BR mutant and control mice of either sex between postnatal day 9 (P9; day of birth was considered to be P0) and P11 for IHC recording. P12–P16 mice were used for OHC recordings. We chose P9–P11 mice for IHC recordings because ACh sensitivity has been shown to be maximal at this stage (Katz et al., 2004; Roux et al., 2011). To study the MOC–OHC synapse, we used P12–P16 mice because OHCs start to be innervated by the MOC fibers at the second postnatal week (Simmons, 2002). In addition, at P12–P16 the cochlear amplifier (OHC electromotility) is already functional (He and Dallos, 1999).

The cochlear preparations were placed in the chamber for electrophysiological recordings, mounted under an Zeiss Axioskop microscope and viewed with differential interference contrast using a 40× water-immersion objective and a camera with contrast enhancement (Dage-MTI). All experimental protocols were performed in accordance with the American Veterinary Medical Association *AVMA Guidelines for the Euthanasia of Animals* (June 2007).

Electrophysiological recordings. IHCs and OHCs were identified visually by their characteristic shape and cell capacitance (7–12 pF). The cochlear preparation was continuously superfused by means of a peristaltic pump (Gilson Minipulse 3, with 8 channels, Bioesanco) containing an extracellular saline solution of an ionic composition similar to that of the perilymph as follows (in mM): 155 NaCl, 5.8 KCl, 1.3 CaCl_2, 0.7 NaH_2PO_4, 5.6 D-glucose, and 10 HEPES buffer, pH 7.4. Working solutions containing the different drugs and toxins were made up in this same saline and delivered through the perfusion system. The pipette solution was as follows (in mM): 150 KCl, 3.5 MgCl_2, 0.1 CaCl_2, 5 EGTA, 5 HEPES buffer, and 2.5 Na_2ATP, pH 7.2. Some cells were removed to access IHCs and OHCs, but mostly the pipette moved through the tissue using positive fluid flow to clear the tip. Currents in IHCs and OHCs were recorded in the whole-cell patch-clamp mode using an Axopatch 200A amplifier,

low-pass filtered at 2–10 kHz and digitized at 5–20 kHz with a Digidata 1322A board (Molecular Devices). Recordings were made at room temperature (22–25°C). Glass pipettes, 1.2 mm inner diameter, had resistances of 7–10 MΩ. Recordings in OHCs were always performed at −40 mV, since at this membrane potential, stable whole-cell recordings and a good signal-to-noise ratio of the outward-going synaptic currents can be obtained (Ballestero et al., 2011). Recordings in IHCs were performed at −90 mV with the exception of those in response to exogenously applied ACh in which IHCs were voltage-clamped both at −90 and at −40 mV. An outward-going current in response to ACh is expected at −40 mV as the ACh current is composed of an inward current flowing through the α9α10 nAChRs [reversal potential (E_{rev}) = −14 mV], plus the more prominent outward current through the Ca^{2+}-activated SK2 potassium channel (E_{rev} = −82 mV). At −90 mV, currents through these two channels are inward (Oliver et al., 2000; Gómez-Casati et al., 2005; Ballestero et al., 2011; Katz et al., 2011). The indicated holding potentials were not corrected for liquid junction potentials (−4 mV). Solutions containing ACh or GABA (Fig. 1) were applied by a gravity-fed multichannel glass pipette (150 μm tip diameter) positioned at ∼300 μm from the recorded IHC or OHC.

Electrical stimulation of MOC efferent axons. Neurotransmitter release was evoked by bipolar electrical stimulation of the medial olivocochlear efferent axons as previously described (Goutman et al., 2005; Zorrilla de San Martín et al., 2010). Briefly, the electrical stimulus was delivered via a 20- to 80-μm-diameter theta glass pipette placed at 20–60 μm modiolar to the base of the recorded IHC or at the base of the IHC that was aligned with the OHC under study. The position of the pipette was adjusted until postsynaptic currents in the IHCs or OHCs (voltage-clamped at −90 or −40 mV, respectively) were consistently activated. An electrically isolated constant current source (model DS3, Digitimer Ltd) was triggered via the data acquisition computer to generate pulses up to 30 mA for 200–2000 μs.

Estimation of the quantum content of transmitter release. The quantum content of transmitter release (*m*) was estimated as the ratio between the mean amplitude of evoked (eIPSCs) and the mean amplitude of spontaneous IPSCs (sIPSCs; Del Castillo and Katz, 1954). To estimate the eIPSC mean amplitude, 200 stimuli were applied at a frequency of 1 Hz. sIPSCs were recorded during and after these 200 stimuli.

The percentage of quantum content (% *m*) after applying a drug or toxin was calculated as follows:

$$\frac{mt}{mc} \times 100,$$

where *mc* is the estimation of *m* in the control condition before drug application to a given cell, and *mt* is the quantum content estimated after incubation of the preparation with the drug or toxin under study for the time specified in the Results section (treated preparations). The variability in quantum content along the experiment in the absence of drug (considered as the control for each experiment, Control % *m*), was calculated comparing the quantum content at 10 min with that at 5 min after break-in for each cell and expressed as a percentage.

As the frequency of sIPSCs is extremely low in OHCs (Ballestero et al., 2011), *m* was calculated by the failures method (*mf* = ln N/N0), where N0 is the number of failures and *N* is the total number of successive trials (200 trials at a frequency of 1 Hz; Hubbard et al., 1969). Failures of release were computed in the absence or presence of the different drugs or toxins.

Statistical significance was evaluated by paired Student's *t* test (one-tailed) unless otherwise stated. A *p* < 0.05 was considered significant. All data were expressed as the mean ± SEM. Synaptic currents were analyzed with Minianalysis (Synaptosoft) and Clampfit 9.2 (Molecular Devices).

Cochlear immunohistochemistry. Whole cochleae were dissected and immediately perfused through the round window with 4% paraformaldehyde (PFA) in PBS, pH 7.4. Cochleae were fixed in 4% PFA overnight at 4°C before rinsing with PBS. Apical turns of the organs of Corti were excised from the cochleae and blocked in blocking buffer (PBS with 5% normal goat serum and 0.3% Triton X-100) for 2 h at room temperature. Cochlear apical turns were incubated with the primary antibody diluted
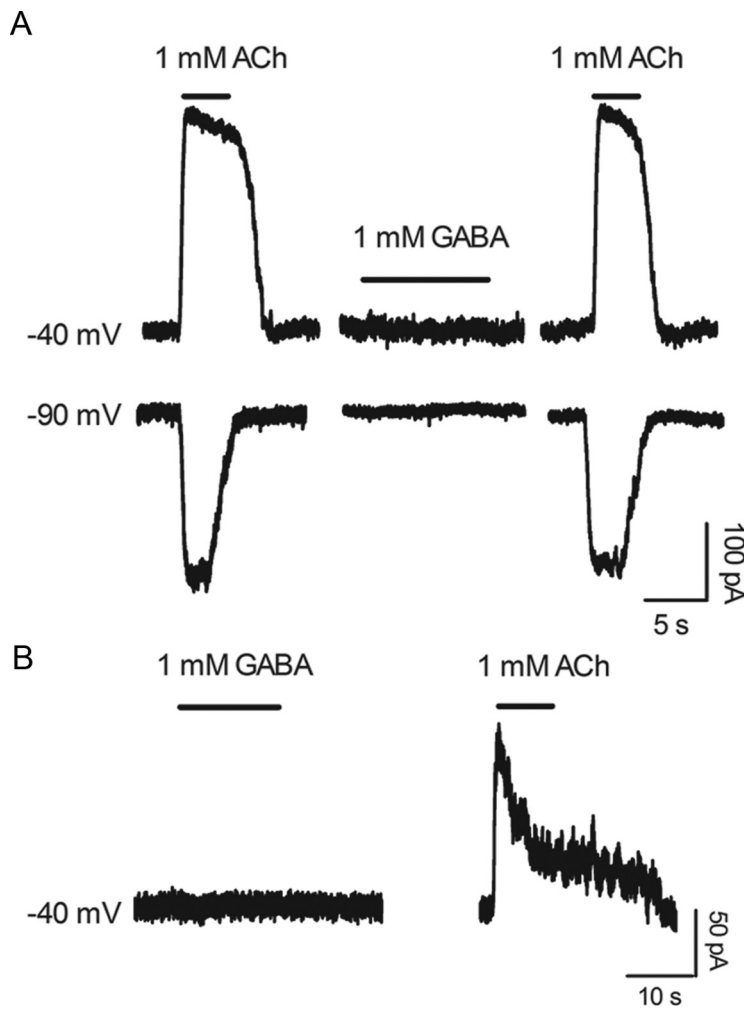
A

B

Figure 1. Effects of exogenously applied GABA to cochlear hair cells. *A*, Representative records obtained in IHCs at P9–P11 upon application of GABA and ACh; 1 mM GABA failed to evoke currents at either −40 or −90 mV in all IHCs tested. ACh, used as a positive control, evoked currents at both potentials in all evaluated IHCs. *B*, Representative records obtained in OHCs at P12–P14 upon application of GABA and ACh. In OHCs, 1 mM GABA failed to evoke currents at −40 mV in all cells tested, whereas ACh evoked currents in all evaluated cells. (Note that OHCs were voltage-clamped at −40 mV and IHCs at both −90 and −40 mV; see Materials and Methods for a detailed explanation of ACh-evoked currents.)

in blocking buffer overnight at 4°C, rinsed three times for 20 min in PBT (PBS with 0.3% Triton X-100), incubated with the secondary antibody diluted in blocking buffer overnight at 4°C, rinsed three times for 20 min in PBT, and rinsed in PBS before mounting on glass slides in Vectashield mounting medium (Vector Laboratories). A laser scanning confocal microscope (Fluoriview, Olympus) was used to acquire images of the whole mounted organs of Corti.

The following antibodies were used: rabbit anti-GFP (1:1000; Invitrogen), rabbit anti-glutamic acid decarboxylase (GAD; 1:500; Synaptic Systems), mouse anti-synaptophysin (1:1000; Millipore), and secondary Alexa Fluor 488- and 568-labeled antibodies (1:1000; Invitrogen).

Drugs and toxins. Stock solutions of peptide toxins were prepared in water. Drugs and reagents were from Sigma-Aldrich, ω-conotoxin-GVIA was from Alomone Labs; and ω-agatoxin-IVA (ω-AgaIVA) was from Peptides International Inc.. All drugs and toxins were thawed and diluted in the extracellular solution shortly before use.

Results
Effects of exogenously applied GABA to OHCs and IHCs
We first evaluated whether GABA is able to elicit postsynaptic currents in mouse cochlear hair cells. GABA (1 mM) was applied, via a gravity-fed perfusion system, to voltage-clamped IHCs and

OHCs in the cochlear preparation. As a positive control, we applied 1 mM ACh to all evaluated cells (Fig. 1).

In P9–P11 IHCs, the age within the short period at which these cells are innervated by MOC efferent fibers (Glowatzki and Fuchs, 2000; Simmons, 2002; Katz et al., 2004; Guinan, 2011; Roux et al., 2011) and at which both the number of functionally innervated cells and their sensitivity to ACh are maximal (Katz et al., 2004; Roux et al., 2011), 1 mM GABA failed to elicit a postsynaptic current ($n = 3$ cells, two mice; Fig. 1A) when voltage-clamped at −40 mV. As under our recording conditions the equilibrium potential for Cl⁻ (E_{Cl-}) is 0 mV, we also tested the effects of GABA at −90 mV, which would enhance a potential current carried by chloride ions. As shown in the bottom of Figure 1A, GABA also failed to elicit currents in IHCs voltage-clamped at this potential. In the same cells 1 mM ACh evoked robust currents at the two holding potentials tested (226.6 ± 50.2 pA at −40 mV, $n = 3$; and -231.7 ± 18.8 pA at −90 mV, $n = 4$; Fig. 1A).

OHCs (P12–P16), the final targets of MOC efferent innervation (Simmons et al., 1996; Simmons, 2002), also lacked responses to 1 mM GABA when voltage-clamped at −40 mV. In the same cells, 1 mM ACh consistently evoked robust outward currents (129.0 ± 21.84 pA; $n = 15$ cells, 12 mice; Fig. 1B). The effects of GABA in OHCs were only tested at −40 mV because these cells became very leaky and unstable at −90 mV (Ballestero et al., 2011). These results clearly show that IHCs and OHCs, at ages at which they are functionally innervated by MOC efferent fibers, lack any GABA_A receptor-mediated responses.

Transmitter release at the MOC–IHC synapse is modified by GABA_B receptor compounds
In view of the lack of postsynaptic responses to exogenously applied GABA in hair cells, we asked whether GABA activates presynaptic GABA_B Rs to inhibit ACh release. Thus, we tested the effects of GABA_B R-selective drugs on the quantum content of transmitter release. Cholinergic postsynaptic responses evoked with single shocks, at a stimulation frequency of 1 Hz, were measured in P9–P11 IHCs voltage-clamped at −90 mV. The quantum content of evoked release (m) was obtained by calculating the mean eIPSC amplitude in every cell and dividing it by the mean sIPSC amplitude (Del Castillo and Katz, 1954). Under our recording conditions, m was 1.2 ± 0.2 ($n = 22$ cells, 21 mice), a value similar to that reported previously in IHCs from both rat (Goutman et al., 2005) and mouse (Zorrilla de San Martín et al., 2010) cochlear preparations. The quantum content of evoked release, evaluated by 200 stimuli given at 1 Hz each 5 min, remained constant during at least 60 min (data not shown). A 5–7 min incubation of the cochlear preparation with 1 μM baclofen, a

selective GABA$_B$R agonist (Misgeld et al., 1995), significantly reduced the amplitude of eIPSCs (control: 39.7 ± 6.1 pA, 1192 events, 8 cells, 6 mice; baclofen: 19.4 ± 2.4 pA, 614 events, 8 cells, 7 mice; unpaired Student's t test, $p < 0.01$; Fig. 2A), without affecting the amplitude of sIPSCs (control: 11.0 ± 0.9 pA, 1651 events; baclofen: 12.0 ± 1.6 pA, 759 events, $p = 0.24$; Fig. 2A, right, inset). Under these conditions, m was reduced to 74.4 ± 6.9% and 57.07 ± 8.3% of the initial value ($p < 0.05$), in the presence of 0.3 and 1 μM baclofen, respectively [control: 126.6 ± 12.3% for 0.3 μM baclofen, 6 cells, 6 mice; and 91.2 ± 7.1% for 1 μM baclofen, 8 cells, 7 mice; Fig. 2B (the bars for the respective control groups are not shown); see Materials and Methods for explanation of how % m was calculated for both control and treated preparations]. As illustrated in Figure 2C, baclofen significantly reduced m in the eight cells tested (control: 1.53 ± 0.32; 1 μM baclofen: 0.87 ± 0.23; $p < 0.01$).

These results suggest that GABA regulates the amount of ACh released at the MOC–IHC synapse through the activation of GABA$_B$R. To further test this hypothesis, we studied the effects of CGP35348, a selective GABA$_B$R antagonist (Bittiger et al., 1993; Fig. 3). CGP35348, at a concentration of 1 μM, significantly increased the amplitude of eIPSCs after 5–7 min of incubation (control: 25.4 ± 11.6 pA, 617 events; CGP35348: 28.5 ± 5.9 pA, 664 events, 6 cells, 6 mice; $p < 0.05$; Fig. 3A) without affecting the amplitude of sIPCS (control: 14.85 ± 0.49 pA, 558 events; CGP35348: 13.5 ± 0.93 pA, $p = 0.08$, 311 events; Fig. 3A, right, inset). Consistent with this result, and in agreement with a presynaptic site of action of CGP35348, m was significantly increased by 1 μM CGP35348 (control: 101.5 ± 12.9%; CGP35348: 147.7 ± 18%; 6 cells, 6 mice; $p < 0.05$; Fig. 3B). The summary plots in Figure 3C show the six cells tested, where 1 μM CGP35348 significantly increased m (control: 1.02 ± 0.41; CGP35348: 1.3 ± 0.45; 6 cells, 6 mice; $p < 0.05$). The fact that both baclofen and CGP35348, the GABA$_B$R agonist and antagonist, respectively, significantly modified the quantum content of evoked release, strongly suggests that GABA inhibits the release of ACh through the activation of presynaptic GABA$_B$R.

Baclofen failed to modify evoked transmitter release at the MOC–IHC synapse in mice lacking functional GABA$_B$Rs

To further explore the involvement of GABA$_B$R in the release of ACh from MOC
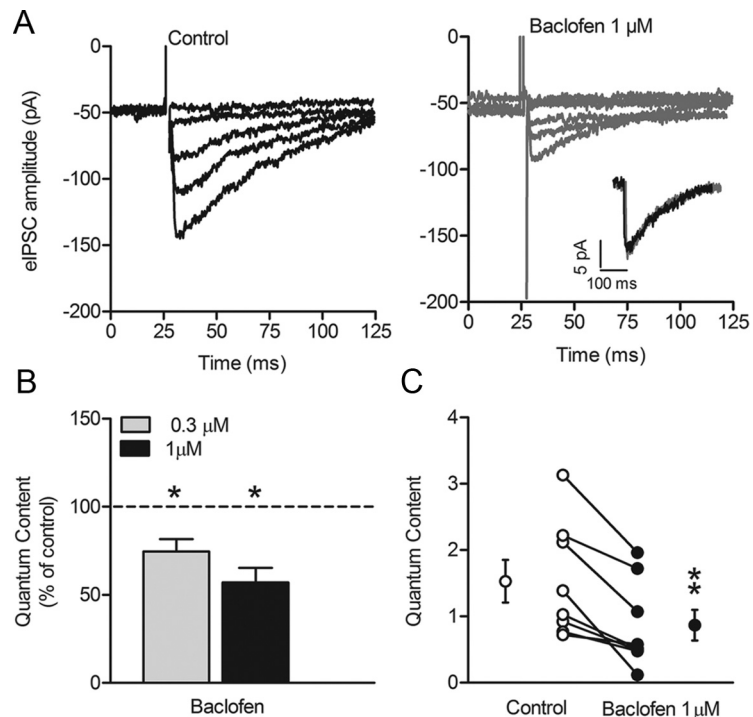

Figure 2. Baclofen, a specific GABA$_B$R agonist, reduces the quantum content of eIPSCs at the MOC–IHC synapse. **A**, Representative traces of eIPSCs recorded at a holding potential of −90 mV before (left) and after 5 min of incubation with 1 μM baclofen (right). The inset in **A** (right) shows that 1 μM baclofen (gray) did not affect the amplitude of sIPSCs. **B**, Bar graph showing that baclofen (0.3 and 1 μM) caused a significant reduction in m. Results are expressed as a percentage of control. **C**, Summary plot for individual cells recorded before (open circles) and after 5 min of incubation with 1 μM baclofen (filled circles). The mean ± SEM values obtained before and after incubation with baclofen are plotted to the left and to the right of their respective individual responses. *$p < 0.05$, **$p < 0.01$, paired Student's t test.
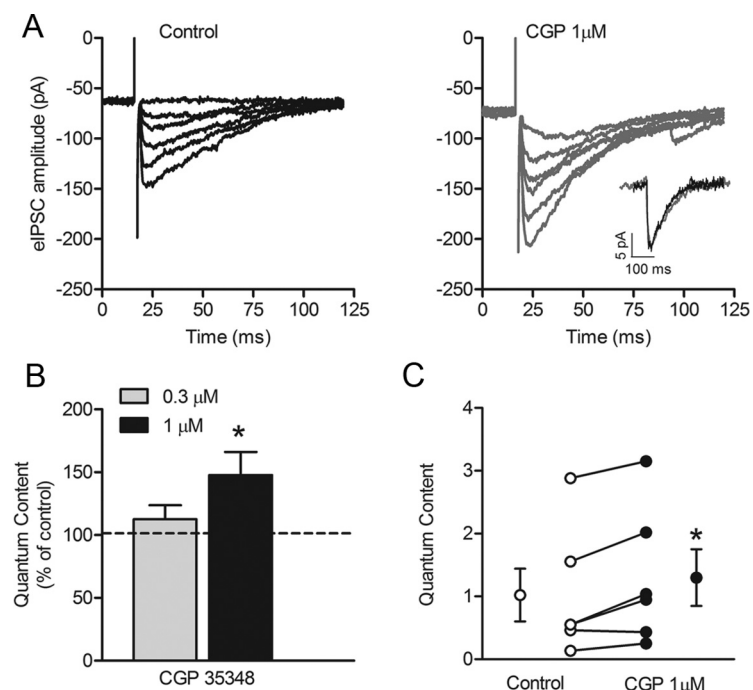

Figure 3. CGP35348, a specific GABA$_B$R antagonist, increases the quantum content of eIPSCs at the MOC–IHC synapse. **A**, Representative traces of eIPSCs recorded at a holding potential of −90 mV before (left) and after 5 min of incubation with 1 μM CGP35348 (right). The inset in **A** (right) shows that 1 μMCGP35348 (gray) did not affect the amplitude of sIPSCs. **B**, Bar graph showing that CGP35348 caused a significant enhancement in m only at a concentration of 1 μM. Results are expressed as a percentage of control. **C**, Summary plot for individual cells recorded before (open circles) and after 5 min of incubation with 1 μM CGP35348 (filled circles). The mean ± SEM values of m obtained before and after incubation with GCP35348 are plotted to the left and to the right of their respective individual responses. *$p < 0.05$, paired Student's t test.
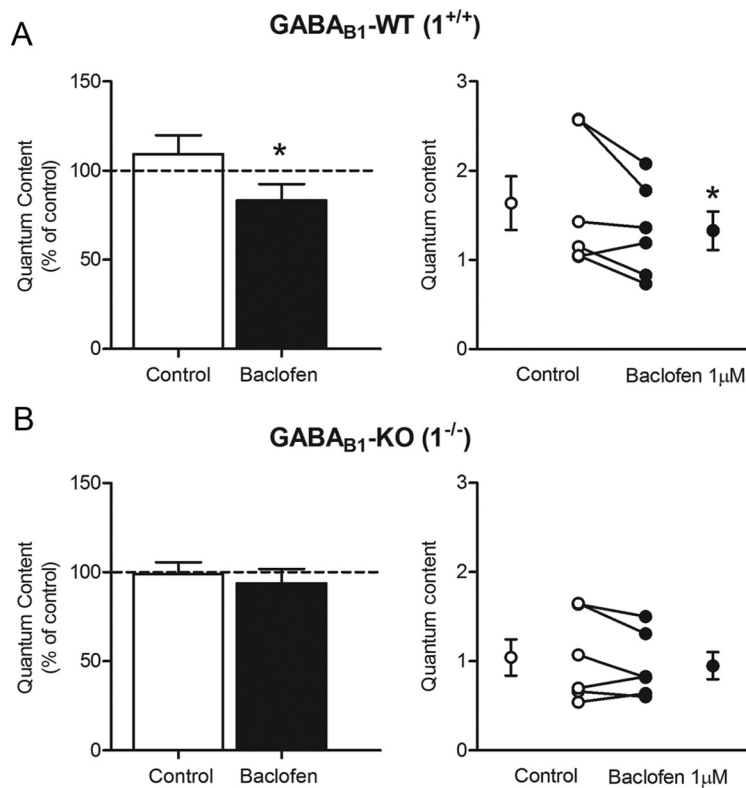
Figure 4. Baclofen fails to reduce the quantum content of eIPSCs at the MOC–IHC synapse in mice lacking functional GABA$_B$Rs. **A, B**, Left, Bar graphs showing that 1 μM baclofen reduced m in wild-type mice (1 $^{+/+}$, **A**) but not in mice lacking functional GABA$_B$Rs (1 $^{-/-}$, **B**). Results are expressed as a percentage of control. **A, B**, Right, Summary plots for individual cells recorded before (open circles) and after 5 min of incubation with 1 μM baclofen (filled circles) in 1 $^{+/+}$ (**A**) and 1 $^{-/-}$ mice (**B**). The mean ± SEM values of m obtained before and after incubation with baclofen are plotted to the left and to the right of their respective individual responses. *$p <$ 0.05 paired Student's t test.

efferent fibers contacting IHCs, we studied the effects of baclofen in GABA$_{B1}$ knock-out (1 $^{-/-}$) mice lacking functional GABA$_B$Rs (Schuler et al., 2001; Bettler et al., 2004; Gassmann et al., 2004; Gassmann and Bettler, 2012). Application of 1 μM baclofen significantly reduced m in wild-type (1 $^{+/+}$) mice (Fig. 4A, left; control: 109.4 ± 10.4%; baclofen: 83.3 ± 9.2%; 6 cells, 6 mice; $p <$ 0.05), but not in 1 $^{-/-}$ littermate mice (Fig. 4B, left; control: 99.0 ± 6.5%; baclofen: 93.8 ± 8.1%; 6 cells, 6 mice; $p =$ 0.32). No significant differences were found in either sIPSC or eIPSC amplitude between wild-type and 1 $^{-/-}$ mice (data not shown). The summary plots for individual cells illustrate that 1 μM baclofen significantly reduced m in 1 $^{+/+}$ mice (control: 1.63 ± 0.3; baclofen: 1.33 ± 0.21; 6 cells; $p <$ 0.05; Fig. 4A, right). However, baclofen did not modify transmitter release (control: 1.04 ± 0.20; baclofen: 0.95 ± 0.16; 6 cells; $p =$ 0.13) in 1 $^{-/-}$ mice (Fig. 4B, right). This result further supports the hypothesis that GABA inhibits transmitter release at the MOC–IHC synapse by acting through presynaptic GABA$_B$Rs.

GABA inhibits the release of ACh at the MOC–IHC synapse through presynaptic GABA$_{B(1a,2)}$Rs

Functional GABA$_B$Rs are heterodimers composed of the GABA$_{B1}$ and GABA$_{B2}$ subunits (Jones et al., 1998; Kaupmann et al., 1998; White et al., 1998; Kuner et al., 1999). Molecular diversity of GABA$_B$R arises from two different and pharmacologically indistinguishable GB1 isoforms, 1a and 1b (Bettler et al., 2004). There is evidence indicating that these two isoforms are expressed at different synaptic sites, with GB1a predominantly located at the

presynapse and GB1b at the postsynapse (Pérez-Garci et al., 2006; Vigot et al., 2006).

To determine which GB1 isoform is involved in the inhibition of ACh release at the MOC–IHC synapse, we compared the effects of baclofen in mutant mice lacking either the GABA$_{B1a}$ (1a $^{-/-}$) or the GABA$_{B1b}$ (1b $^{-/-}$) isoform (Vigot et al., 2006; Fig. 5). Application of 1 μM baclofen significantly reduced m at MOC–IHC synapses from wild-type littermate mice of both isoforms (1a $^{+/+}$: Fig. 5A, left; control: 94.3 ± 10.1%; baclofen: 64.6 ± 8.8%; 10 cells, 8 mice; $p <$ 0.05; 1b $^{+/+}$: Fig. 5C, left; control: 102.5 ± 8.1%; baclofen: 72.9 ± 4.2%; 7 cells, 7 mice; $p <$ 0.01). Baclofen did not modify m in 1a $^{-/-}$ mice (Fig. 5B, left; control: 106.3 ± 7.0%; baclofen: 96.9 ± 6.8%; 13 cells, 9 mice; $p =$ 0.09), indicating that the GABA$_{B1a}$ isoform inhibits transmitter release. On the contrary, m was significantly reduced in 1b $^{-/-}$ mice, excluding an involvement of the GABA$_{B1b}$ isoform (Fig. 5D, left; control: 113.4 ± 10.5%; baclofen: 70.7 ± 10.0%; 7 cells, 6 mice; $p <$ 0.01). The right panels in Figure 5A–D are the summary plots for individual cells from each group of mice recorded in control conditions and after 7 min of incubation with 1 μM baclofen (Fig. 5A, 1a $^{+/+}$: control, 1.60 ± 0.2; baclofen, 1.04 ± 0.21; 10 cells; $p <$ 0.01; Fig. 5B, 1a $^{-/-}$: control, 1.56 ± 0.25; baclofen, 1.54 ± 0.27; 13 cells; $p =$ 0.46; Fig. 5C, 1b $^{+/+}$: control, 1.33 ± 0.2; baclofen, 0.92 ± 0.1; 7 cells; $p <$ 0.01; Fig. 5D, 1b $^{-/-}$: control, 1.5 ± 0.3; baclofen, 1.03 ± 0.27; 7 cells; $p <$ 0.01). Baclofen did not alter the amplitude of sIPSCs in any of the GABA$_B$R knock-out mice (data not shown). Together, our results strongly suggest that ACh release at the MOC–IHC synapse is inhibited by GABA acting on presynaptic GABA$_{B1a}$-containing receptors, the GABA$_{B(1a,2)}$Rs.

P/Q-type VGCCs are inhibited following GABA$_B$R activation

We have recently shown that both P/Q- and N-type VGCCs support neurotransmitter release at the mouse MOC–IHC synapse before the onset of hearing (Zorrilla de San Martín et al., 2010). To gain insight into the mechanisms underlying the inhibition that GABA exerts on ACh release at this synapse, we tested the effects of the GABA$_B$ antagonist CGP35348 in the presence of blockers of P/Q- and N-type VGCCs, ω-AgaIVA, and ω-conotoxin GVIA (ω-CgTx), respectively.

As previously reported (Zorrilla de San Martín et al., 2010), m was greatly reduced after 15 min of incubation with 200 nM ω-AgaIVA (Fig. 6A,B; control: 1.20 ± 0.14; 9 cells, 9 mice; ω-AgaIVA: 0.26 ± 0.1; 11 cells, 9 mice; $p <$ 0.001). Under this condition, CGP35348 failed to significantly increase the amount of transmitter released by the MOC fibers (Fig. 6A,B; +CGP: 0.34 ± 0.1; 9 cells, 9 mice; $p =$ 0.07). The inset in Figure 6 shows representative averaged traces illustrating the effects of ω-AgaIVA and CGP35348 on the amplitude of eIPSCs. sIPSCs were not affected by either of these drugs (data not illustrated; control: 9.33 ± 0.4 pA; ω-AgaIVA: 8.6 ± 0.3 pA; +CGP: 8.4 ±
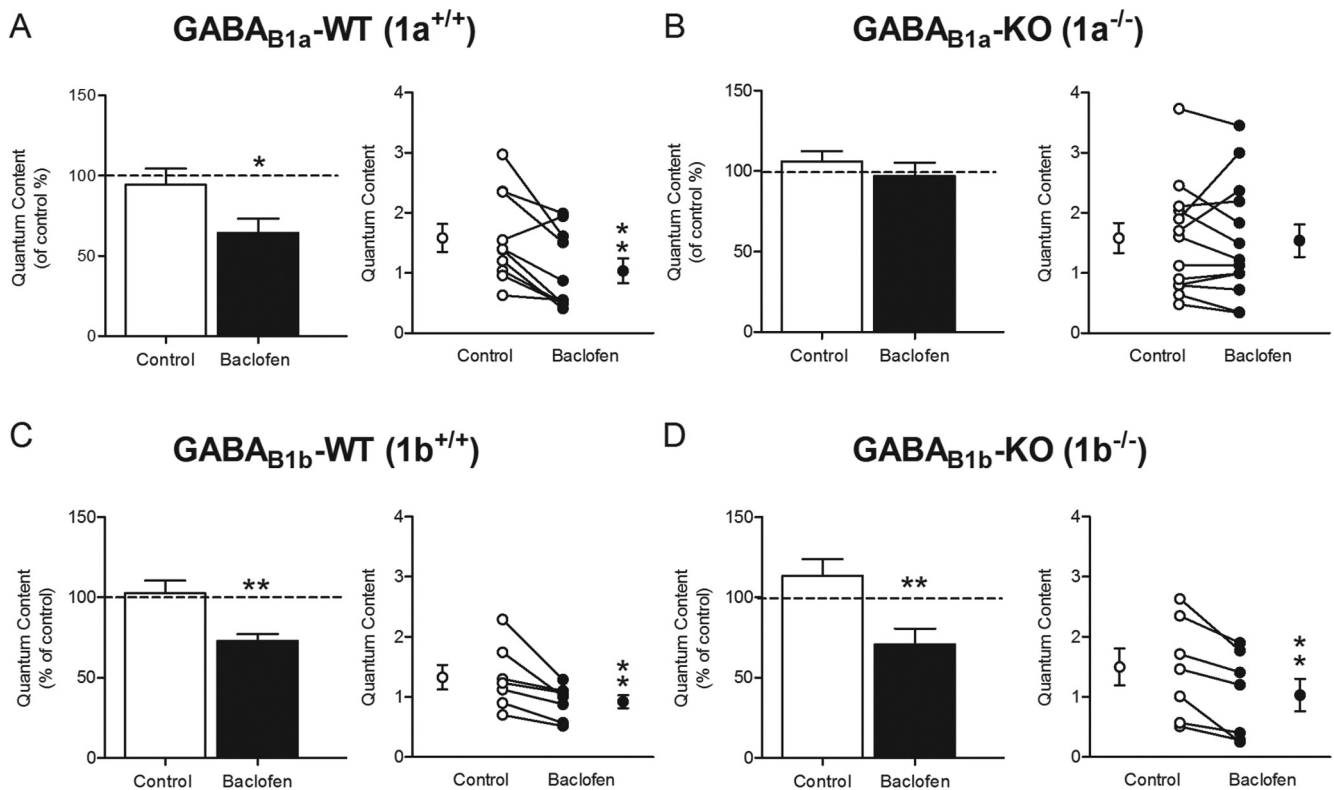
Figure 5. Baclofen fails to reduce the quantum content of eIPSCs at the MOC–IHC synapse in mice lacking the 1a GABA_BR isoform. ***A–D***, Quantum content of eIPSC recorded in IHCs, evoked by electrical stimulation of the MOC efferent axons before and after incubation with 1 μM baclofen in wild-type (***A***, ***C***) and in isoform-specific GABA_B knock-out mice: 1a$^{-/-}$ in ***B***; 1b$^{+/+}$ in ***D***. In the bar graphs, results are expressed as a percentage of control. Summary plots for individual cells recorded before and after 7 min of incubation with 1 μM baclofen are shown on the right in ***A–D***. The mean ± SEM values of m obtained before and after incubation with baclofen are plotted to the left and to the right of their respective individual responses. *$p < 0.05$, **$p < 0.01$, paired Student's t test.

0.4 pA; 9 cells, 9 mice; ANOVA, $p = 0.17$; $n = 179$, 123, and 104 events, respectively).

Figure 6D and E, shows that m was, as previously reported (Zorrilla de San Martín et al., 2010) significantly reduced after 15 min of incubation with 500 nM ω-CgTx (control: 0.73 ± 0.1; 7 cells, 7 mice; ω-CgTx; 0.35 ± 0.1; 13 cells, 11 mice; $p < 0.001$). Under this condition, 1 μM CGP35348 was still able to significantly increase m when compared with the ω-CgTx-treated group (+CGP: 0.51 ± 0.1; 10 cells, 8 mice; $p < 0.05$). Figure 6, inset, shows representative averaged traces illustrating the effect of ω-CgTx and CGP35348 on the amplitude of eIPSPs. sIPSC amplitude was not affected by ω-CgTx or ω-CgTx+CGP (data not illustrated; control: 11.1 ± 0.2 pA; ω-CgTx: 11.5 ± 0.3 pA; +CGP: 10.9 ± 0.2 pA; 7 cells, 7 mice; ANOVA, $p = 0.21$, $n = 300$, 210, and 185 events, respectively). Together, these results suggest that the activity of P/Q-type VGCCS is reduced following GABA_BR activation.

GABA regulates the release of ACh at the MOC–OHCs synapse through inhibitory presynaptic GABA_BRs
At the beginning of the second postnatal week, OHCs begin to respond to ACh (Dulon and Lenoir, 1996; He and Dallos, 1999). To determine whether GABA exerts an inhibitory effect on ACh release at these synapses, we tested the effects of the GABA_BR antagonist CGP35348 on the quantum content of evoked release at the MOC–OHC synapse (Fig. 7). As the frequency of sIPSCs at MOC–OHC synapses is very low, m was evaluated by the failures method (see Materials and Methods).

Representative traces of eIPSCs recorded in OHCs (P14) before (Fig. 7A) and after (Fig. 7B) incubating the cochlear preparation with 1 μM CGP35348 show that the number of failures decreased in the presence of the antagonist. Consistently, ACh release was significantly enhanced in the presence of the antagonist (Fig. 7C; control: 111.0 ± 26.6%; CGP35348: 170.4 ± 37.5%; 4 cells, 3 mice; $p < 0.05$). The summary plot in Figure 7D shows that m significantly increased in the four cells tested after incubating the cochlear preparation with CGP35348 (control: 0.12 ± 0.02; CGP35348: 0.29 ± 0.04; $p < 0.01$). These results indicate that GABA inhibits ACh release at the MOC–OHC synapse through the activation of presynaptic GABA_BRs. In a future work, experiments will be carried out to test whether ACh release at the MOC–OHC synapse is also inhibited by GABA acting on presynaptic GABA_{B(1a,2)}Rs.

GABA_BRs are expressed in efferent synaptic terminals at the base of IHCs and OHCs before the onset of hearing
The electrophysiological experiments shown above demonstrate that synaptic activation of GABA_BRs inhibits ACh release at both MOC–IHC and MOC–OHC synapses. To confirm the expression of GABA_BRs at the terminals of these synapses, we used a transgenic mouse line (GABA_{B1}-GFP) in which GFP is fused to the GABA_{B1} subunit (Casanova et al., 2009; Fig. 8). Cochlear whole-mount preparations from P9–P14 were coimmunostained with GFP antibodies to enhance the endogenous GFP signal and to detect GFP-tagged GABA_{B1} subunits and synaptophysin antibodies to identify efferent terminals contacting hair
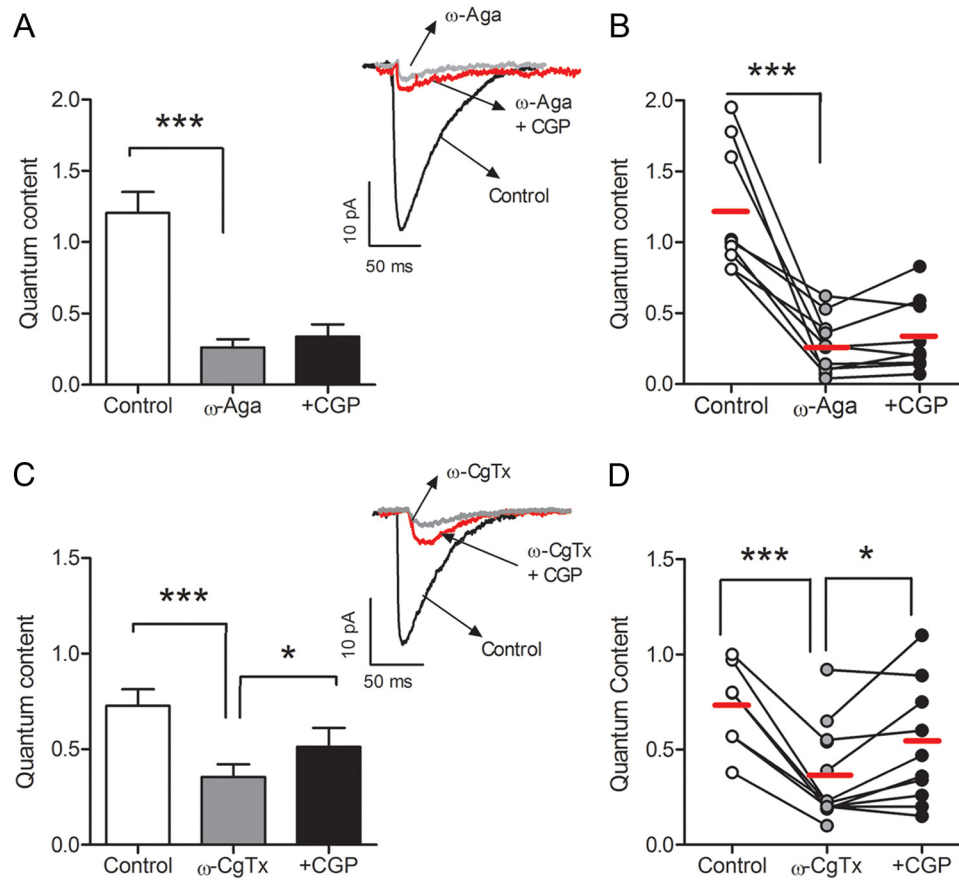
Figure 6. P/Q-type Ca^{2+} channels are the target of GABA$_B$ receptor activation at the transient MOC–IHC synapse. **A**, **B**, Bar diagram (**A**) and the plot of individual cells (**B**) show the effects of 1 μM CGP35348 on m after blocking P/Q-type VGCCs with 200 nM ω-agatoxin-IVA. Inset between **A** and **B** illustrates representative averaged traces showing the effects of CGP on the amplitude of eIPSPs in the presence of ω-agatoxin-IVA (control, black; ω-Aga, gray; +CGP, red). **C, D**, Bar diagram (**C**) and plot of individual cells (**D**) illustrating the effect of 1 μM CGP35348 on transmitter release after blocking N-type VGCCs with 500 nM ω-conotoxin GVIA. Inset between graphs illustrates representative averaged traces showing the effects of CGP35348 on the amplitude of eIPSPs in the presence of ω-conotoxin GVIA (control, black; ω-CgTx, gray; +CGP, red). Red horizontal bars in **B** and **D** represent the mean in each group. Error bars represent the SEM. *$p < 0.05$, ***$p < 0.001$, paired Student's t test.

cells. A GABA$_{B1}$-GFP-positive signal was detected in the inner spiral bundle region at the base of IHCs containing both efferent and type I afferent neurons. A strong colocalization of GFP with synaptophysin was observed, indicating the presence of GABA$_B$Rs at efferent terminals under the IHCs (Fig. 8A–C). In the OHC region, GABA$_{B1}$ expression was found both in type II afferent and MOC efferent fibers contacting the OHCs (Fig. 8C, inset, filled arrow). The expression of GABA$_B$Rs at MOC terminals suggests the presence of the neurotransmitter GABA at the synapse. To study whether GABA is present at efferent terminals contacting hair cells at ages around the onset of hearing, we used an antibody that recognizes the GABA synthetic enzyme GAD (Fig. 8D–F) together with an antibody recognizing synaptophysin. In regions below IHCs and OHCs, GAD colocalized with synaptophysin (Fig. 8F, inset, filled arrow). These immunostainings are consistent with our electrophysiological results showing that GABA is involved in the modulation of synaptic transmission at MOC–hair cell efferent synapses during development.

Discussion
Lack of GABA postsynaptic effects
The present results show that GABA failed to elicit postsynaptic currents in either OHCs or IHCs. This suggests that, at least in mid-apical cochlear turns from P9–P16 mice, there are no functional postsynaptic GABA$_A$ receptors at either the MOC–OHC or

the MOC–IHC synapse. The discrepancy with a report showing that application of GABA hyperpolarizes OHCs (Gitter and Zenner, 1992) might be explained by differences in species (guinea pigs vs mice) and/or age (adult vs P12–P16) of the animals used in the experiments. The absence of postsynaptic GABA$_A$-mediated responses is consistent with the observation that when the α9α10 nAChR is pharmacologically blocked, no postsynaptic currents in response to either K$^+$ elevation or electrical stimulation of the MOC efferent axons are seen in OHCs (Oliver et al., 2000; Ballestero et al., 2011) and IHCs (Glowatzki and Fuchs, 2000). Moreover, it is in line with the finding that in α9 knock-out mice, no postsynaptic currents are left (Vetter et al., 2007), clearly indicating that fast synaptic transmission at the OC–hair synapse is cholinergic and mediated only through the α9α10 nAChR (Fig. 9). Moreover, the fact that GABA$_B$ receptors are not expressed either in postnatal (present work) or adult hair cells (Maison et al., 2009) further suggests a lack of a postsynaptic GABA$_B$-mediated action. Together, these results support the idea that the main effect of the profuse OC GABAergic innervation that makes direct synaptic contacts with cochlear hair cells is not a postsynaptic one.

GABA modulates transmitter release at MOC–hair cell synapses through GABA$_{B(1a,2)}$Rs
The results obtained with the GABA$_B$R agonist and antagonist indicate that GABA inhibits ACh release at MOC–hair cell

synapses through presynaptic GABA_BRs. These results are in agreement with the classical role of GABA in presynaptic modulation of synaptic transmission at mammalian glutamatergic and GABAergic synapses via heteroreceptors and autoreceptors, respectively (Gaiarsa et al., 1995; Brenowitz et al., 1998; Chalifoux and Carter, 2011; Fischl et al., 2012). The modulation of ACh release, as described in the present work, although not widely observed, is not without precedent. For example, the activation of presynaptic GABA_BRs inhibits ACh release from *Caenorhabditis elegans* motoneurons (Schultheis et al., 2011) and from cholinergic nerve terminals in the rat superior cervical ganglion (Farkas et al., 1986). However, the present results are unique due to the inhibitory sign of the cholinergic OC–hair cell synapse. Thus, the release of GABA at the inhibitory mammalian cholinergic synapse activates presynaptic GABA_BRs that inhibit the release of ACh and therefore curtail inhibition.

The lack of effect of baclofen in mice with a specific ablation in the GB1a (1a^{-/-}) subunit isoform (Vigot et al., 2006) clearly demonstrates the involvement of the GB1a isoform in the presynaptic inhibition of ACh release at the MOC–IHC synapse. This is in agreement with the established role of GABA_{B1a} in presynaptic inhibition (Gassmann and Bettler, 2012). For example, at glutamatergic hippocampal CA3–CA1 synapses, GABA_{B1a} mainly assembles into presynaptic heteroreceptors, while receptors formed by the GABA_{B1b} subunit mediate postsynaptic inhibition (Vigot et al., 2006). Similarly, presynaptic inhibition at GABAergic synapses between synaptic terminals from neurons in cortical layer 1 and pyramidal neurons in cortical layer 5 is absent in the 1a^{-/-} but not in the 1b^{-/-} mice, suggesting that GABA_{B1a} but not GABA_{B1b} subunits assemble into presynaptic autoreceptors (Pérez-Garci et al., 2006). Our findings at a cholinergic synapse thus provide further evidence for distinct physiological roles and a differential distribution of GABA_{B1} subunit isoforms.

GABA_BRs negatively regulate synaptic transmission at the MOC–IHC synapse by inhibiting P/Q-type VGCCs

At the MOC–IHC synapse, ACh release is mediated by both N- and P/Q-type VGCCs (Zorrilla de San Martín et al., 2010). At several central synapses, presynaptic GABA_BRs reduce transmitter release by direct inhibition of P/Q- and N-type VGCCs through Gβγ subunits of the activated G-protein (Mintz and Bean, 1993; Thompson et al., 1993; Lambert and Wilson, 1996; Bowery et al.,
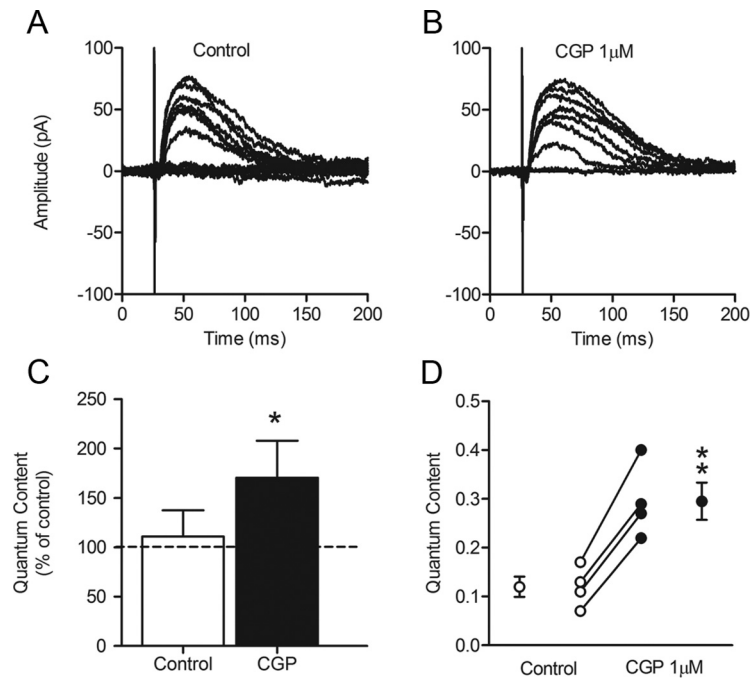

Figure 7. CGP35348 increases the quantum content of transmitter release at the MOC–OHC synapse. **A, B**, Representative traces of eIPSCs recorded in OHCs at −40 mV, before and after incubation with 1 μM CGP35348. **C**, Bar diagram showing that CGP35348 (1 μM) significantly increased *m* at the MOC–OHC synapse. Results are expressed as a percentage of control. **D**, Summary plot for individual cells recorded before and after 15 min of incubation with 1 μM CGP35348. The mean ± SEM values of *m* obtained before and after incubation with CGP35348 are plotted to the left and to the right of their respective individual responses. *$p < 0.05$, **$p < 0.01$, paired Student's *t* test.
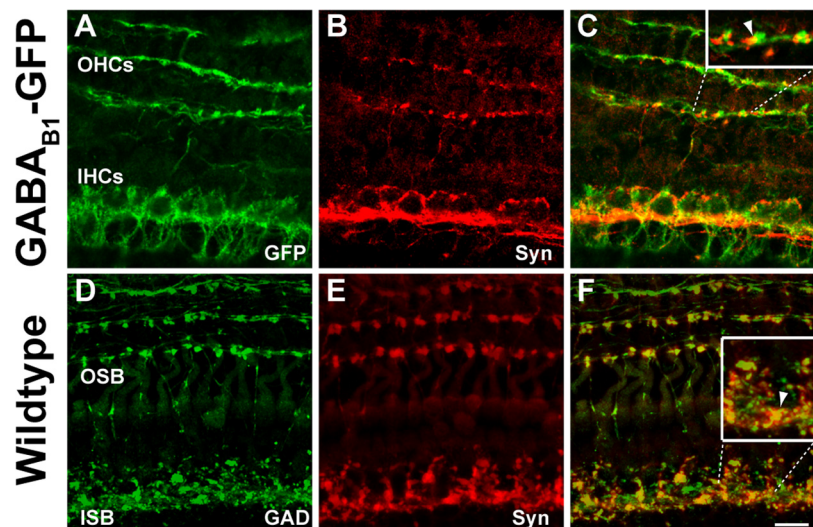

Figure 8. GABA_BRs are expressed in efferent synaptic terminals at the base of IHCs and OHCs. **A–C**, Cochlear wholemount preparations from P9 to P14 double-immunostained with anti-GFP; **A**, green), and synaptophysin (Syn; **B**, red). A strong colocalization of GFP with synaptophysin can be observed (**C**, yellow) in the inner spiral bundle region at the base of IHCs (efferent and type I afferent neurons) and, at the OHC region, in type II afferent and MOC efferent fibers contacting the cells (**C**, filled arrow). **D–F**, cochlear preparations from similar aged mice immunostained with an antibody to the GABA synthetic enzyme GAD (**D**, green) together with synaptophysin (**E**, red). **F**, Immunoreactivity is visible as small puncta below IHCs (filled arrow) and OHCs indicating that GAD colocalized with synaptophysin at these regions (yellow). ISN, Inner spiral bundle; OSB, outer spiral bundle.

2002; Bettler et al., 2004). The fact that the GABA_BRs antagonist CGP35348 failed to significantly increase transmitter release at the MOC–IHC synapse when P/Q-type VGCCs were completely blocked by ω-agatoxin-IVA, together with the observation that CGP353548 increased transmitter release after blocking N-type
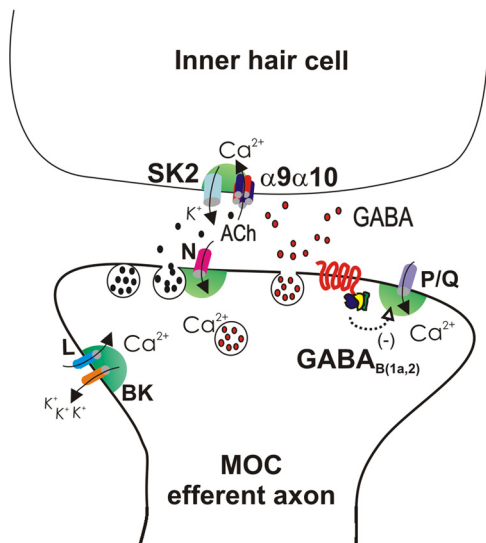
Figure 9. Schematic representation of the ion channels and receptors that support and regulate transmitter release from the MOC efferent synaptic terminals. After invasion of the terminal action potential, Ca^{2+} entering through both P/Q- and N-type VGCCs supports the release of ACh, while L-type VGCCs exert a negative control on this process by activating BK channels (Zorrilla de San Martín et al., 2010). The present results strongly suggest that GABA, coreleased with ACh, activates presynaptic GABA_{B(1a,2)}Rs, which negatively regulate the release of ACh by altering Ca^{2+} influx through P/Q-type VGCCs.

VGCCs with ω-conotoxin GVIA, indicates that P/Q- and not N-type VGCCs are inhibited by GABA_BR activation (Fig. 9). However, our results do not exclude the participation of other proteins in the GABA_B signaling cascade, like L-type VGCCs (Shen and Slaughter, 1999; Zorrilla de San Martín et al., 2010; Bray and Mynlieff, 2011) and like proteins of the vesicular release machinery downstream of VGCCs (Yoon et al., 2007).

GABA_BRs are expressed in efferent synaptic terminals at the base of IHCs and OHCs
The electrophysiological data suggest the presence of functional GABA_BRs at MOC synaptic terminals contacting both the IHCs and OHCs. Immunostaining experiments in transgenic GABA_{B1}-GFP mice further demonstrate the expression of GABA_BRs in OC terminals contacting these cells. In the IHC area, the GABA_{B1}-GFP immunostaining arising from the OC terminals could, in principle, derive from the LOC fibers contacting type I afferent dendrites, the MOC fibers that transiently innervate the IHCs, or both (Liberman et al., 1990; Vetter et al., 1991; Simmons, 2002; Maison et al., 2003). Our electrophysiological data, however, rule out the possibility that GABA_BRs are solely expressed in the LOC fibers innervating the afferent neurons and clearly demonstrate that functional GABA_BRs are present at the MOC synaptic terminals making axo-somatic synapses with IHCs.

The lack of GFP immunostaining in OHCs and IHCs, and the presence of GFP immunostaining in type I and type II afferent fibers in GABA_{B1}-GFP mice during development replicate the findings that were made with adult mice (Maison et al., 2009). In addition, this agrees with the presence of GABA_BR transcripts in mouse spiral ganglion neurons from embryonic through adult stages (Lin et al., 2000). Interestingly, in adult mice, GABA_BRs were not detected in OC efferent terminals in either the IHC or the OHC areas (Maison et al., 2009). Together, the present results and those of Maison et al. (2009) suggest that the OC efferent

synaptic terminals transiently express GABA_BRs. Moreover, the results imply that GABA_BRs are expressed in type I and type II afferent fibers before the onset of hearing and remain there through adulthood. In contrast, GABA_BRs expressed in OC terminals are downregulated between the onset of hearing and adulthood. Downregulation of GABA_BR during development, most prominently the GABA_{B1a} isoform, has been described (Malitschek et al., 1998; Bianchi et al., 2005). Interestingly, the expression of two postsynaptic key molecules of the transient MOC–IHC synapse, the α10 nAChR subunit and the SK2 K^+ channel, also cease to express around the onset of hearing (Katz et al., 2004), further highlighting the importance of cochlear synaptic refinement during the critical period (Simmons et al., 1996).

Functional consequences
Our functional data, together with the immunodetection of GABA_B receptors at OC terminals and of GAD in fibers reveal the existence of GABAergic OC fibers contacting IHCs and OHCs around the onset of hearing. These results are in agreement with the notion that the only source of GABAergic input to the mammalian cochlea is the OC system (Fex and Altschuler, 1986; Thompson et al., 1986; Vetter et al., 1991; Eybalin, 1993; Maison et al., 2003). Moreover, our functional data suggest that GABA and ACh are both released upon MOC fiber activity (Fig. 9). Based on the observations that in adult mice GABA and ACh are colocalized in the same terminals (Maison et al., 2003), we hypothesize that both neurotransmitters are coreleased upon efferent activation. Corelease of GABA and ACh, two fast neurotransmitters of usually opposite excitability, from the same terminal has been described for the retinal starburst amacrine cells (Duarte et al., 1999; Lee et al., 2010), where both neurotransmitters act at postsynaptic receptors. However, a different scenario is observed at the OC–hair synapse, where ACh release might be regulated by coreleased GABA acting at GABA_B autoreceptors.

Presynaptic inhibition of ACh release via GABA_BRs might shape short-term plasticity properties of the MOC–hair cell synapses by regulating the release probability and, thus, as reported for other synapses (Brenowitz et al., 1998; Brenowitz and Trussell, 2001), allow continuous signaling upon high-frequency MOC activity. Since MOC firing frequency increases with sound intensity (Robertson and Gummer, 1985; Brown, 1989) and the efficacy of the MOC–IHC synapse is optimal when MOC fibers are activated at high frequency (Ballestero et al., 2011), presynaptic inhibition might therefore be relevant for MOC protection from acoustic trauma (Rajan, 2000; Taranda et al., 2009).

Conclusions
Synaptic strength is a key variable during development for both establishing and refining connections. Our results show that during the development of the auditory system GABA inhibits the amount of ACh released at the MOC–hair cell synapse through presynaptic GABA_{B(1a,2)}Rs, coupled to P/Q-type VGCCS. Thus, we demonstrate that GABA regulates the strength of the MOC–IHC synapse, and could thereby control the IHC firing frequency, and, therefore, the release of glutamate in the first auditory synapse at a critical period where synaptic connections are actively being formed in the cochlea, also a period where the entire auditory pathway is being established.

References

Ballestero J, Zorrilla de San Martín J, Goutman J, Elgoyhen AB, Fuchs PA, Katz E (2011) Short-term synaptic plasticity regulates the level of olivocochlear inhibition to auditory hair cells. J Neurosci 31:14763–14774. CrossRef Medline

Batta TJ, Panyi G, Szucs A, Sziklai I (2004) Regulation of the lateral wall stiffness by acetylcholine and GABA in the outer hair cells of the guinea pig. Eur J Neurosci 20:3364–3370. CrossRef Medline

Bettler B, Kaupmann K, Mosbacher J, Gassmann M (2004) Molecular structure and physiological functions of GABA(B) receptors. Physiol Rev 84:835–867. CrossRef Medline

Beutner D, Moser T (2001) The presynaptic function of mouse cochlear inner hair cells during development of hearing. J Neurosci 21:4593–4599. Medline

Bianchi MS, Lux-Lantos VA, Bettler B, Libertun C (2005) Expression of gamma-aminobutyric acid B receptor subunits in hypothalamus of male and female developing rats. Brain Res Dev Brain Res 160:124–129. CrossRef Medline

Bittiger H, Froestl W, Mickel S, Olpe HR (1993) GABAB receptor antagonists: from synthesis to therapeutic applications. Trends Pharmacol Sci 14:391–394. CrossRef Medline

Bowery NG, Bettler B, Froestl W, Gallagher JP, Marshall F, Raiteri M, Bonner TI, Enna SJ (2002) International Union of Pharmacology. XXXIII. Mammalian gamma-aminobutyric acid(B) receptors: structure and function. Pharmacol Rev 54:247–264. CrossRef Medline

Bray JG, Mynlieff M (2011) Involvement of protein kinase C and protein kinase A in the enhancement of L-type calcium current by GABAB receptor activation in neonatal hippocampus. Neuroscience 179:62–72. CrossRef Medline

Brenowitz S, Trussell LO (2001) Minimizing synaptic depression by control of release probability. J Neurosci 21:1857–1867. Medline

Brenowitz S, David J, Trussell L (1998) Enhancement of synaptic efficacy by presynaptic GABA(B) receptors. Neuron 20:135–141. CrossRef Medline

Brown MC (1989) Morphology and response properties of single olivocochlear fibers in the guinea pig. Hear Res 40:93–109. CrossRef Medline

Casanova E, Guetg N, Vigot R, Seddik R, Julio-Pieper M, Hyland NP, Cryan JF, Gassmann M, Bettler B (2009) A mouse model for visualization of GABA(B) receptors. Genesis 47:595–602. CrossRef Medline

Chalifoux JR, Carter AG (2011) GABAB receptor modulation of synaptic function. Curr Opin Neurobiol 21:339–344. CrossRef Medline

Del Castillo J, Katz B (1954) Quantal components of the end-plate potential. J Physiol 124:560–573. Medline

Duarte CB, Santos PF, Carvalho AP (1999) Corelease of two functionally opposite neurotransmitters by retinal amacrine cells: experimental evidence and functional significance. J Neurosci Res 58:475–479. CrossRef Medline

Dulon D, Lenoir M (1996) Cholinergic responses in developing outer hair cells of the rat cochlea. Eur J Neurosci 8:1945–1952. CrossRef Medline

Elgoyhen A, Vetter D, Katz E, Rothlin C, Heinemann S, Boulter J (2001) Alpha 10: a determinant of nicotinic cholinergic receptor function in mammalian vestibular and cochlear mechanosensory hair cells. Proc Natl Acad Sci U S A 98:3501–3506. CrossRef Medline

Eybalin M (1993) Neurotransmitters and neuromodulators of the mammalian cochlea. Physiol Rev 73:309–373. Medline

Farkas Z, Kása P, Balcar VJ, Joó F, Wolff JR (1986) Type A and B GABA receptors mediate inhibition of acetylcholine release from cholinergic nerve terminals in the superior cervical ganglion of rat. Neurochem Int 8:565–572. CrossRef Medline

Fex J, Altschuler RA (1986) Neurotransmitter-related immunocytochemistry of the organ of Corti. Hear Res 22:249–263. CrossRef Medline

Fischl MJ, Combs TD, Klug A, Grothe B, Burger RM (2012) Modulation of synaptic input by GABAB receptors improves coincidence detection for computation of sound location. J Physiol 590:3047–3066. CrossRef Medline

Gaiarsa JL, Tseeb V, Ben-Ari Y (1995) Postnatal development of pre- and postsynaptic GABAB-mediated inhibitions in the CA3 hippocampal region of the rat. J Neurophysiol 73:246–255. Medline

Gassmann M, Bettler B (2012) Regulation of neuronal GABA(B) receptor functions by subunit composition. Nat Rev Neurosci 13:380–394. CrossRef Medline

Gassmann M, Shaban H, Vigot R, Sansig G, Haller C, Barbieri S, Humeau Y, Schuler V, Müller M, Kinzel B, Klebs K, Schmutz M, Froestl W, Heid J,

Kelly PH, Gentry C, Jaton AL, Van der Putten H, Mombereau C, Lecourtier L, et al (2004) Redistribution of GABA_{B(1)} protein and atypical GABA_B responses in GABA_{B(2)}-deficient mice. J Neurosci 24:6086–6097. CrossRef Medline

Gitter AH, Zenner HP (1992) gamma-Aminobutyric acid receptor activation of outer hair cells in the guinea pig cochlea. Eur Arch Otorhinolaryngol 249:62–65. Medline

Glowatzki E, Fuchs PA (2000) Cholinergic synaptic inhibition of inner hair cells in the neonatal mammalian cochlea. Science 288:2366–2368. CrossRef Medline

Gómez-Casati ME, Fuchs PA, Elgoyhen AB, Katz E (2005) Biophysical and pharmacological characterization of nicotinic cholinergic receptors in rat cochlear inner hair cells. J Physiol 566:103–118. CrossRef Medline

Goutman JD, Fuchs PA, Glowatzki E (2005) Facilitating efferent inhibition of inner hair cells in the cochlea of the neonatal rat. J Physiol 566:49–59. CrossRef Medline

Guinan JJ (2011) Physiology of the medial and lateral olivocochlear systems. In: Auditory and vestibular efferents (Ryugo DK, Fay RR, Popper AN, eds), pp 39–81. New York: Springer.

He DZ, Dallos P (1999) Development of acetylcholine-induced responses in neonatal gerbil outer hair cells. J Neurophysiol 81:1162–1170. Medline

Hubbard JI, Llinás RR, Quastel DMJ (1969) Electrophysiological analysis of synaptic transmission. London: Edward Arnold.

Johnson SL, Eckrich T, Kuhn S, Zampini V, Franz C, Ranatunga KM, Roberts TP, Masetto S, Knipper M, Kros CJ, Marcotti W (2011) Position-dependent patterning of spontaneous action potentials in immature cochlear inner hair cells. Nat Neurosci 14:711–717. CrossRef Medline

Jones KA, Borowsky B, Tamm JA, Craig DA, Durkin MM, Dai M, Yao WJ, Johnson M, Gunwaldsen C, Huang LY, Tang C, Shen Q, Salon JA, Morse K, Laz T, Smith KE, Nagarathnam D, Noble SA, Branchek TA, Gerald C (1998) GABA(B) receptors function as a heteromeric assembly of the subunits GABA(B)R1 and GABA(B)R2. Nature 396:674–679. CrossRef Medline

Katz E, Elgoyhen AB, Gómez-Casati ME, Knipper M, Vetter DE, Fuchs PA, Glowatzki E (2004) Developmental regulation of nicotinic synapses on cochlear inner hair cells. J Neurosci 24:7814–7820. CrossRef Medline

Katz E, Elgoyhen AB, Fuchs PA (2011) Cholinergic inhibition of hair cells. In: Auditory and vestibular efferents (Ryugo DK, Fay RR, Popper AN, eds), pp 103–133. New York: Springer.

Kaupmann K, Malitschek B, Schuler V, Heid J, Froestl W, Beck P, Mosbacher J, Bischoff S, Kulik A, Shigemoto R, Karschin A, Bettler B (1998) GABA(B)-receptor subtypes assemble into functional heteromeric complexes. Nature 396:683–687. CrossRef Medline

Kuner R, Köhr G, Grünewald S, Eisenhardt G, Bach A, Kornau HC (1999) Role of heteromer formation in GABAB receptor function. Science 283:74–77. CrossRef Medline

Lambert NA, Wilson WA (1996) High-threshold Ca2+ currents in rat hippocampal interneurones and their selective inhibition by activation of GABA(B) receptors. J Physiol 492:115–127. Medline

Lee S, Kim K, Zhou ZJ (2010) Role of ACh-GABA cotransmission in detecting image motion and motion direction. Neuron 68:1159–1172. CrossRef Medline

Liberman MC, Dodds LW, Pierce S (1990) Afferent and efferent innervation of the cat cochlea: quantitative analysis with light and electron microscopy. J Comp Neurol 301:443–460. CrossRef Medline

Lin X, Chen S, Chen P (2000) Activation of metabotropic GABAB receptors inhibited glutamate responses in spiral ganglion neurons of mice. Neuroreport 11:957–961. CrossRef Medline

Maison SF, Adams JC, Liberman MC (2003) Olivocochlear innervation in the mouse: immunocytochemical maps, crossed versus uncrossed contributions, and transmitter colocalization. J Comp Neurol 455:406–416. CrossRef Medline

Maison SF, Rosahl TW, Homanics GE, Liberman MC (2006) Functional role of GABAergic innervation of the cochlea: phenotypic analysis of mice lacking GABA_A receptor subunits α1, α2, α5, α6, β2, β3, or δ. J Neurosci 26:10315–10326. CrossRef Medline

Maison SF, Casanova E, Holstein GR, Bettler B, Liberman MC (2009) Loss of GABA(B) receptors in cochlear neurons: threshold elevation suggests modulation of outer hair cell function by type II afferent fibers. J Assoc Res Otolaryngol 10:50–63. CrossRef Medline

Malitschek B, Rüegg D, Heid J, Kaupmann K, Bittiger H, Fröstl W, Bettler B, Kuhn R (1998) Developmental changes of agonist affinity at GABABR1

receptor variants in rat brain. Mol Cell Neurosci 12:56–64. CrossRef Medline

Mintz IM, Bean BP (1993) GABAB receptor inhibition of P-type Ca2+ channels in central neurons. Neuron 10:889–898. CrossRef Medline

Misgeld U, Bijak M, Jarolimek W (1995) A physiological role for GABAB receptors and the effects of baclofen in the mammalian central nervous system. Prog Neurobiol 46:423–462. CrossRef Medline

Oliver D, Klöcker N, Schuck J, Baukrowitz T, Ruppersberg JP, Fakler B (2000) Gating of Ca2+-activated K+ channels controls fast inhibitory synaptic transmission at auditory outer hair cells. Neuron 26:595–601. CrossRef Medline

Pérez-Garci E, Gassmann M, Bettler B, Larkum ME (2006) The GABAB1b isoform mediates long-lasting inhibition of dendritic Ca2+ spikes in layer 5 somatosensory pyramidal neurons. Neuron 50:603–616. CrossRef Medline

Rajan R (2000) Centrifugal pathways protect hearing sensitivity at the cochlea in noisy environments that exacerbate the damage induced by loud sound. J Neurosci 20:6684–6693. Medline

Robertson D, Gummer M (1985) Physiological and morphological characterization of efferent neurones in the guinea pig cochlea. Hear Res 20:63–77. CrossRef Medline

Roux I, Wersinger E, McIntosh JM, Fuchs PA, Glowatzki E (2011) Onset of cholinergic efferent synaptic function in sensory hair cells of the rat cochlea. J Neurosci 31:15092–15101. CrossRef Medline

Schuler V, Lüscher C, Blanchet C, Klix N, Sansig G, Klebs K, Schmutz M, Heid J, Gentry C, Urban L, Fox A, Spooren W, Jaton AL, Vigouret J, Pozza M, Kelly PH, Mosbacher J, Froestl W, Käslin E, Korn R, et al (2001) Epilepsy, hyperalgesia, impaired memory, and loss of pre- and postsynaptic GABA(B) responses in mice lacking GABA(B(1)). Neuron 31:47–58. CrossRef Medline

Schultheis C, Brauner M, Liewald JF, Gottschalk A (2011) Optogenetic analysis of GABAB receptor signaling in Caenorhabditis elegans motor neurons. J Neurophysiol 106:817–827. CrossRef Medline

Shen W, Slaughter MM (1999) Metabotropic GABA receptors facilitate L-type and inhibit N-type calcium channels in single salamander retinal neurons. J Physiol 516:711–718. CrossRef Medline

Simmons DD (2002) Development of the inner ear efferent system across vertebrate species. J Neurobiol 53:228–250. CrossRef Medline

Simmons DD, Mansdorf NB, Kim JH (1996) Olivocochlear innervation of inner and outer hair cells during postnatal maturation: evidence for a waiting period. J Comp Neurol 370:551–562. CrossRef Medline

Taranda J, Maison SF, Ballestero JA, Katz E, Savino J, Vetter DE, Boulter J, Liberman MC, Fuchs PA, Elgoyhen AB (2009) A point mutation in the hair cell nicotinic cholinergic receptor prolongs cochlear inhibition and enhances noise protection. PLoS Biol 7:e18. CrossRef Medline

Thompson GC, Cortez AM, Igarashi M (1986) GABA-like immunoreactivity in the squirrel monkey organ of Corti. Brain Res 372:72–79. CrossRef Medline

Thompson SM, Capogna M, Scanziani M (1993) Presynaptic inhibition in the hippocampus. Trends Neurosci 16:222–227. CrossRef Medline

Vetter DE, Adams JC, Mugnaini E (1991) Chemically distinct rat olivocochlear neurons. Synapse 7:21–43. CrossRef Medline

Vetter DE, Katz E, Maison SF, Taranda J, Turcan S, Ballestero J, Liberman MC, Elgoyhen AB, Boulter J (2007) The alpha10 nicotinic acetylcholine receptor subunit is required for normal synaptic function and integrity of the olivocochlear system. Proc Natl Acad Sci U S A 104:20594–20599. CrossRef Medline

Vigot R, Barbieri S, Bräuner-Osborne H, Turecek R, Shigemoto R, Zhang YP, Luján R, Jacobson LH, Biermann B, Fritschy JM, Vacher CM, Müller M, Sansig G, Guetg N, Cryan JF, Kaupmann K, Gassmann M, Oertner TG, Bettler B (2006) Differential compartmentalization and distinct functions of GABAB receptor variants. Neuron 50:589–601. CrossRef Medline

White JH, Wise A, Main MJ, Green A, Fraser NJ, Disney GH, Barnes AA, Emson P, Foord SM, Marshall FH (1998) Heterodimerization is required for the formation of a functional GABA(B) receptor. Nature 396:679–682. CrossRef Medline

Yoon EJ, Gerachshenko T, Spiegelberg BD, Alford S, Hamm HE (2007) Gbetagamma interferes with Ca2+-dependent binding of synaptotagmin to the soluble N-ethylmaleimide-sensitive factor attachment protein receptor (SNARE) complex. Mol Pharmacol 72:1210–1219. CrossRef Medline

Zenner HP, Gitter AH, Rudert M, Ernst A (1992) Stiffness, compliance, elasticity and force generation of outer hair cells. Acta Otolaryngol 112:248–253. Medline

Zorrilla de San Martín J, Pyott S, Ballestero J, Katz E (2010) Ca2+ and Ca2+-activated K+ channels that support and modulate transmitter release at the olivocochlear efferent-inner hair cell synapse. J Neurosci 30:12157–12167. CrossRef Medline